PERGAMON

International Journal of Solids and Structures 39 (2002) 3811–3830

INTERNATIONAL JOURNAL OF SOLIDS and STRUCTURES

www.elsevier.com/locate/ijsolstr

On modelling phase propagation in SMAs by a Maxwellian thermo-viscoelastic approach

Cristian Făciu *, Mihaela Mihăilescu-Suliciu

Institute of Mathematics of the Romanian Academy, P.O. Box 1-764, RO-70700 Bucharest, Romania

Received 13 February 2002

Abstract

In this paper we propose a Maxwellian thermo-viscoelastic approach to the problem of phase transformation in shape memory alloys. An explicit temperature-dependent non-monotone piecewise linear stress–strain relation is considered and the corresponding free energy function is used to establish the heat propagation equation. The heat exchange between the material and its environment is also taken into account. The numerical simulations of three end-displacement rates lead to serrated hysteresis loops and result in inhomogeneous deformations and exothermic/endothermic behavior during loading/unloading tests. It is shown that the influence of the strain rate on the size and shape of the hysteresis loop is due in fact to the heat exchange between the bar and its environment. The predictions are compared qualitatively with experimental results. © 2002 Elsevier Science Ltd. All rights reserved.

Keywords: Non-convex free energy; Phase transition; Thermo-viscoelasticity; Austenite; Martensite

1. Introduction

A great deal of effort has been devoted in the last four-decade history of shape memory alloys (SMAs) within both mechanics and metallurgy communities to the understanding and modelling of two remarkable properties of these materials: the shape memory effect and the pseudoelastic behavior. It is well known that a phase transformation between two solid state phases called austenite (A) and martensite (M) is responsible for both effects which can be induced by either changes in temperature or in stress.

Many micromechanical aspects of this material behavior have been elucidated within such efforts, including for example the capture of crystallographic aspects, dislocation microstructures and twin boundaries (see for instance Otsuka and Wayman (1998)). Despite these developments the connection between microscopic and macroscopic behavior is still not fully developed due to the complexity of the problem. Moreover, the variety of new structural applications which exploit the material's special properties requires appropriate phenomenological models able to incorporate relevant micromechanical features.

* Corresponding author. Fax: +40-1-212-5126.
E-mail addresses: cristian.faciu@imar.ro, cfaciu@yahoo.fr (C. Făciu).

0020-7683/02/$ - see front matter
PII: S0020-7683(02)00178-6

There are several viewpoints in the constitutive modelling of these materials and a rich literature on this subject. In the following we shall focus more on the classical one, mainly based on the thermoelasticity theory with multiple energy-wells (or, equivalently with a non-monotone stress–strain relation) for certain ranges of strain and temperature, and on related approaches. In these theories each energy-well is identified with a phase of the material.

Beginning with the paper by Ericksen (1975) there are numerous and important studies which have been carried out in phase transformations that appeal to the minimization of the stored energy of the mixed phases and use subtle mathematical techniques (see for instance Ball and James (1987) and James (1981)) to determine the amount of phases that coexist and the way they are juxtaposed. In fact this approach does not address the process of phase transformation rather it describes the coexistence of the phases after the transformation has taken place. On the other side, if we consider initial and boundary value problems for the corresponding field equations we get ill-posed problems in the sense of Hadamard.

Thus an important and open problem is to find simple and appropriate dissipative mechanisms to be included in the constitutive description of the materials such that the model be able to describe the process of phase transformation, i.e., the nucleation and the propagation of phases.

Such an example is the thermodynamical framework developed by Abeyaratne and Knowles (1993) which in addition to the usual thermoelastic properties contains a nucleation criterion and a kinetic relationship for the motion of the interfaces.

A new approach to the problem of phase transformations or strain localization in materials exhibiting material instabilities has been advanced in a one-dimensional and isothermal context by Suliciu (1989) (see also Făciu, 1991; Suliciu, 1992; Făciu and Suliciu, 1994; Mihăilescu-Suliciu and Suliciu, 1993 and the references therein). This formulation is based on a rate-type viscoelastic constitutive equation with Maxwellian viscosity. Thus one considers the rate of stress, the rate of strain and the over-stress function as being linearly related, while the equilibrium states are situated on a stress–strain curve corresponding to a non-monotone elastic material. This simple rate-dependent constitutive equation has the capability to describe relaxation, creep and instantaneous processes of the material. In fact this approach is equivalent to a model for a simple body with one internal variable (the inelastic strain). Its strain and stress-dependent free energy function is non-convex and its energetical properties were extensively investigated (see Suliciu (1998) and the references therein). Thus one obtains a viscoelastic approach to non-monotone elasticity which no longer leads to ill posed problems since the corresponding PDE system is hyperbolic. The nucleation and growth of one phase into another, the creation and propagation of phase boundaries is automatically accounted for this model. A detailed investigation on the way the dissipation mechanism contained in this model describes the process of nucleation and propagation of phase boundaries can be found in Făciu (1996).

Recent experimental studies of SMAs (Leo et al., 1993; Lin et al., 1994; Shaw and Kyriakides, 1997) have exhibited a strong coupling between their mechanical and thermal properties and have clarified many aspects of their interactions.

In order to model the thermal effects which accompany phase transitions in SMAs we consider in this paper a rate-type semilinear thermo-viscoelastic approach to nonlinear and non-monotone thermoelasticity (a more general framework has been considered by Suliciu (1998)). Moreover we include here the thermo-mechanical coupling of the material with its environment by using a Newton's type convection mode of heat transfer.

The content of this paper is the following. In Section 2 we formulate the balance laws for a one-dimensional setting which take into account the heat exchange of the bar with its surrounding. Section 3 describes the constitutive assumptions and their compatibility with the second law of thermodynamics. Based on the thermo-mechanical properties of SMAs we consider an equilibrium stress–strain-temperature relation related with the one proposed by Abeyaratne et al. (1994). Next, we derive the stress–strain-temperature dependent free energy function of the viscoelastic model as well as the three-well equilibrium energy function. Details are given in Appendices. In Section 4 we carry out a number of simulations and

compare them in detail with the experimental results obtained by Shaw and Kyriakides (1997). The objective of these calculations is to establish how effectively our continuum-type model can reproduce the morphology of deformations and thermal changes observed in experiments. We show that the simulations successfully capture the nucleation and evolution of deformation fronts and the corresponding distribution of the temperature fields observed in laboratory experiments.

A related approach to the isothermal problem of phase transition in solid bodies has been considered by Pego (1987). His formulation is based on a viscoelastic model with Newtonian (or Kelvin–Voight) viscosity for which the rate of strain is proportional with the over-stress function while the equilibrium stress–strain relation is also non-monotone. This rate-type constitutive relation can describe only creep processes, but not relaxation and instantaneous processes. Thus the PDE system which describes the motion of a thin viscoelastic bar is parabolic. The non-convex free energy function of this model is just the free energy function of the associated elastic model, i.e., it is only strain-dependent. The predictions of this model have been investigated by Pego (1987) for a dead-load experiment while the case of strain-controlled problems has been investigated by Vainchtein and Rosakis (1999) (see also the references therein). In a different framework the Newtonian viscoelastic constitutive equation has also been used to establish a particular kinetic relation at the interface between propagating phases (Abeyaratne and Knowles, 1991).

There are many similarities between the viscoelastic Maxwellian and Newtonian approaches of non-monotone elasticity. First, no other supplementary constitutive information in the form of a nucleation criterion or kinetic law is necessary. Both contain a dissipation mechanism which allows the description of nucleation and phase propagation during strain-controlled experiments and exhibit a hysteretic behavior with serrations on the two horizontal branches of the hysteresis loop. In both cases inertia forces have to be included in the field equations as they play an essential role when instability phenomena accompanying phase transition processes develop. An investigation concerning the differences between the predictions of these two models for the same input data should be made. This approach was extended and analyzed by Vainchtein (2001) for the case of temperature-dependent non-monotone equilibrium stress–strain relations, but without considering the thermal changes through the lateral surface of the bar.

2. Basic equations

We consider a thin cylindrical bar of length L, mass density ϱ and constant cross-sectional area (A) with X the coordinate along its symmetry axis in the reference configuration. Assuming that all field quantities are uniform over a cross-section, i.e., they only depend on (X,t) where $t>0$ is time, we consider a purely one-dimensional setting.

The balance of momentum equation for the bar is given by

$$\frac{\mathrm{d}}{\mathrm{d}t}\int_{X_1}^{X_2}\varrho v(X,t)A\,\mathrm{d}X=\int_{X_1}^{X_2}\varrho b(X,t)A\,\mathrm{d}X+\sigma(X_2,t)A-\sigma(X_1,t)A, \tag{1}$$

which must hold for any $X_1,X_2\in[0,L]$, where (v,σ,b) are the particle velocity, the nominal stress (force per unit area in the reference configuration) and the body force per unit mass, respectively.

In order to take into account the heat exchange of the bar with its surrounding we assume that the heat that enters or leaves the specimen through its lateral surface is equal to $-\omega(\theta-\theta_0)$, where $\omega=\text{const.}>0$, is a material parameter, θ being the absolute temperature and θ_0 being the ambient temperature.

Then the balance of energy equation can be written as

$$\frac{\mathrm{d}}{\mathrm{d}t}\int_{X_1}^{X_2}\varrho\left(\frac{v^2}{2}+e\right)A\,\mathrm{d}X=\int_{X_1}^{X_2}\varrho(bv+r)A\,\mathrm{d}X+A(\sigma v-q)(X_2,t)-A(\sigma v-q)(X_1,t)-\int_{\mathscr{A}_{\mathrm{lat}}}\omega(\theta-\theta_0)\,\mathrm{d}s, \tag{2}$$

for any $X_1, X_2 \in [0, L]$, where $\mathscr{A}_{\text{lat}}$ is the lateral surface of the bar between X_1 and X_2, and (e, q, r) are the specific internal energy, the axial heat flux and the heat supply per unit mass, respectively.

The second law of thermodynamics is taken under the form

$$\frac{\mathrm{d}}{\mathrm{d}t}\int_{X_1}^{X_2} \varrho\eta A\,\mathrm{d}X \geqslant \int_{X_1}^{X_2} \frac{\varrho r}{\theta} A\,\mathrm{d}X - A\left(\frac{q}{\theta}\right)(X_2, t) + A\left(\frac{q}{\theta}\right)(X_1, t) - \int_{\mathscr{A}_{\text{lat}}} \frac{\omega(\theta - \theta_0)}{\theta}\,\mathrm{d}s, \tag{3}$$

for any $X_1, X_2 \in [0, L]$, where η is the specific entropy.

The PDE system corresponding to (1)–(3) is therefore

$$\begin{aligned}
&\varrho\frac{\partial v}{\partial t} - \frac{\partial \sigma}{\partial X} = \varrho b,\\
&\frac{\partial \varepsilon}{\partial t} - \frac{\partial v}{\partial X} = 0,\\
&\varrho\frac{\partial e}{\partial t} - \sigma\frac{\partial \varepsilon}{\partial t} + \frac{\partial q}{\partial X} = -\frac{2}{R}\omega(\theta - \theta_0) + \varrho r,\\
&\varrho\frac{\partial \eta}{\partial t} + \frac{\partial}{\partial X}\left(\frac{q}{\theta}\right) \geqslant -\frac{2}{R}\frac{\omega(\theta - \theta_0)}{\theta} + \frac{\varrho r}{\theta},
\end{aligned} \tag{4}$$

with R is the radius of the bar, where we also have considered the compatibility condition $(4)_2$ between strain and velocity fields and R denotes the radius of the bar.

3. Constitutive assumptions

In order to have a complete PDE system describing the thermo-mechanical motion of the bar we need to add to the system (4) a set of constitutive relations for stress σ, internal energy e and axial flux q. Recall we have already made a constitutive assumption by introducing the material parameter ω characterizing the heat exchange with the heat bath surrounding the bar.

In this section we briefly present our continuum thermo-mechanical setting for shape memory bars. The constitutive assumptions considered here are taken from the general constitutive framework presented in Făciu and Mihăilescu-Suliciu (2001a).

We make the following constitutive assumptions:

$$\begin{aligned}
&\frac{\partial \sigma}{\partial t} = E\frac{\partial \varepsilon}{\partial t} - k(\sigma - \sigma_R(\varepsilon, \theta)),\\
&e = \hat{e}(\varepsilon, \theta, \sigma),\\
&q = -\kappa\frac{\partial \theta}{\partial X},
\end{aligned} \tag{5}$$

where $E = \text{const.} > 0$ is the dynamic Young's modulus, $k = \text{const.} > 0$ is a Maxwell type viscosity coefficient (i.e., $1/k$ is a relaxation time of the material) and $\kappa = \text{const.} > 0$ is the heat conductivity coefficient in the Fourier law.

$\sigma = \sigma_R(\varepsilon, \theta)$ is called *the thermoelastic equilibrium surface* and is defined on a domain $D = (\varepsilon_1^*(\theta), \varepsilon_2^*(\theta)) \times (\theta_1^*, \theta_2^*) \subset (-1, \infty) \times (0, \infty)$, where $\varepsilon_1^*(\theta)$ and $\varepsilon_2^*(\theta)$ are two continuous and piecewise smooth functions on (θ_1^*, θ_2^*).

The internal energy function $\hat{e}$ given by $(5)_2$ is defined on a constitutive domain $\tilde{D} \subset (-1, \infty) \times (\theta_1^*, \theta_2^*) \times R$ which requires a detailed characterization presented in Făciu and Mihăilescu-Suliciu (2001a).

The existence of a free energy function $\hat{\psi} = \hat{\psi}(\varepsilon, \theta, \sigma)$ (or entropy function $\hat{\eta} = \hat{\eta}(\varepsilon, \theta, \sigma)$)

$$\psi = \hat{\psi}(\varepsilon, \theta, \sigma) = \hat{e}(\varepsilon, \theta, \sigma) - \theta\hat{\eta}(\varepsilon, \theta, \sigma), \tag{6}$$

results as a requirement of the second law of thermodynamics $(4)_4$ which may also be written in the form

$$\varrho\frac{\partial\psi}{\partial t}\leqslant\sigma\frac{\partial\varepsilon}{\partial t}-\varrho\eta\frac{\partial\theta}{\partial t}-\frac{q}{\theta}\frac{\partial\theta}{\partial X}. \tag{7}$$

We have shown that the constitutive structure (5) has a free energy function $\hat{\psi}=\hat{\psi}(\varepsilon,\theta,\sigma)$ on $\tilde{D}$ compatible with the second law of thermodynamics iff

$$\frac{\partial\hat{\psi}}{\partial\varepsilon}+E\frac{\partial\hat{\psi}}{\partial\sigma}=\frac{\sigma}{\varrho}\quad\text{and}\quad\frac{\partial\hat{\psi}}{\partial\sigma}(\sigma-\sigma_R(\varepsilon,\theta))\leqslant 0. \tag{8}$$

While the entropy function $\hat{\eta}=\hat{\eta}(\varepsilon,\theta,\sigma)$ is given by

$$\hat{\eta}=-\frac{\partial\hat{\psi}}{\partial\theta}. \tag{9}$$

Moreover we have shown in Făciu and Mihăilescu-Suliciu (2001a) (extending our result in Făciu and Mihăilescu-Suliciu (1987)) that the solution $\psi=\hat{\psi}(\varepsilon,\theta,\sigma)$ of the system (8) exists and it is unique (modulo an additive function of temperature) iff

$$\frac{\sigma_R(\varepsilon_1,\theta)-\sigma_R(\varepsilon_2,\theta)}{\varepsilon_1-\varepsilon_2}<E\quad\text{for any }\varepsilon_1\neq\varepsilon_2\in(\varepsilon_1^*(\theta),\varepsilon_2^*(\theta))\text{ and }\theta\in(\theta_1^*,\theta_2^*) \tag{10}$$

and has the form

$$\varrho\hat{\psi}(\varepsilon,\theta,\sigma)=\frac{\sigma^2}{2E}-\frac{\sigma_R^2(\tilde{\varepsilon},\theta)}{2E}+\int_0^{\tilde{\varepsilon}}\sigma_R(s,\theta)\,\mathrm{d}s+\phi(\theta), \tag{11}$$

where $\tilde{\varepsilon}$ is uniquely defined by relation $\sigma-E\varepsilon=\sigma_R(\tilde{\varepsilon},\theta)-E\tilde{\varepsilon}$.

In this approach we construct rather than postulate the thermodynamic potentials starting from the constitutive information available for the equilibrium stress–strain-temperature relation. Therefore, according to (11), all three constitutive functions $(\hat{\psi},\hat{\eta},\hat{e})(\varepsilon,\theta,\sigma)$ are completely determined on $\tilde{D}$ (modulo an additive function of temperature) by the equilibrium surface $\sigma_R(\varepsilon,\theta)$ and the dynamic Young's modulus E. In order to determine the unknown function $\phi(\theta)$ in (11) we need additional information on the thermal behaviour of the material. As usual we assume in this paper that the specific heat at constant strain of the thermoelastic material $\sigma=\sigma_R(\varepsilon,\theta)$ in the austenitic phase is constant (see (B.2)). Let us note that knowing the equilibrium surface and the specific heat at constant strain means knowledge of the equilibrium thermomechanical behavior of the material and the additional knowledge of dynamic Young's modulus E extends only the mechanical properties outside equilibrium. A detailed analysis on this subject is done in Făciu and Mihăilescu-Suliciu (2001a) in a more general framework.

If we denote by $\hat{\psi}_R(\varepsilon,\theta)=\hat{\psi}(\varepsilon,\theta,\sigma_R(\varepsilon,\theta))$ the free energy function at equilibrium and by $\hat{\eta}_R(\varepsilon,\theta)=\hat{\eta}(\varepsilon,\theta,\sigma_R(\varepsilon,\theta))$ the entropy function at equilibrium we find the classical thermostatic relations, i.e.,

$$\sigma_R(\varepsilon,\theta)=\rho\frac{\partial\hat{\psi}_R}{\partial\varepsilon}(\varepsilon,\theta)\quad\text{and}\quad\hat{\eta}_R(\varepsilon,\theta)=-\frac{\partial\hat{\psi}_R}{\partial\theta}(\varepsilon,\theta). \tag{12}$$

It is known that for the one-dimensional theory the bulk behavior of a thermoelastic material which can describe phase transitions phenomena is characterized by stress–strain-temperature relations which are non-monotone with respect to strain for certain ranges of temperature, or equivalently by non-convex free energy functions in strain for the same temperature intervals. It is obvious that condition (10) on the constitutive functions entering $(5)_1$ allows us to consider such equilibrium stress–strain-temperature relations. A simple example will be considered in the following. For our thermo-viscoelastic model whenever the equilibrium free-energy function $\hat{\psi}_R(\varepsilon,\theta)$ is non-convex with respect to strain on certain intervals of

temperature the strain–stress-temperature dependent free energy function $\hat{\psi}(\varepsilon,\sigma,\theta)$ is also non-convex but with respect to $(\sigma - E\varepsilon)$ for the corresponding ranges of temperature.

It is useful to note that the balance of energy equation $(4)_3$ can be written now only by means of the free energy function, as

$$\varrho\theta\frac{\partial^2\hat{\psi}}{\partial\theta^2}\frac{\partial\theta}{\partial t} = -\kappa\frac{\partial^2\theta}{\partial X^2} - k\varrho\frac{\partial\hat{\psi}}{\partial\sigma}(\sigma-\sigma_R(\varepsilon,\theta)) + k\varrho\theta\frac{\partial^2\hat{\psi}}{\partial\theta\partial\sigma}(\sigma-\sigma_R(\varepsilon,\theta)) + \frac{2\omega}{R}(\theta-\theta_0) \tag{13}$$

and relations $(4)_{1,2}$, $(5)_1$ and (13) form a complete PDE system for the unknown functions $(v,\varepsilon,\theta,\sigma)$.

The first term in the right-hand side of the heat propagation equation (13) describes the thermal dissipation through axial conduction, the second one the internal dissipation, the third one is related with the latent heat released or absorbed by the material while the last one gives account on the gain or loss of heat across the lateral surface of the bar.

We propose now an explicit stress–strain-temperature relation $\sigma = \sigma_R(\varepsilon,\theta)$ that characterizes the response of a three-phase material. The thermo-elastic equilibrium surface we consider here is very close to that derived from physical considerations on the behavior of shape memory alloys by Abeyaratne et al. (1994), but there are differences which will be pointed out in the following.

Thus, we consider a material which exists in a high-temperature phase austenite (A) and has two variants (M^-) and (M^+) of a low-temperature phase martensite. The thermo-mechanical assumptions we consider here are the following. There are two critical temperatures $\theta_m > \theta_1^*$ and $\theta_M < \theta_2^*$ such as, for $\theta > \theta_M$ the material only exists in its austenite form no matter what the stress level is, whereas for $\theta < \theta_m$ the material only exists in its martensitic forms. For $\theta \in [\theta_m,\theta_M]$ all three phases are available to the material.

The stress response function σ_R must therefore be a monotonically increasing function of ε for $\theta > \theta_M$. At each temperature $\theta \in [\theta_m,\theta_M]$ as the strain increases we require $\sigma_R(\cdot,\theta)$ to increase too for $\varepsilon \in (\varepsilon_1^*(\theta),\varepsilon_m^-(\theta)) \cup (\varepsilon_M^-(\theta),\varepsilon_M^+(\theta)) \cup (\varepsilon_m^+(\theta),\varepsilon_2^*(\theta))$ and to decrease over the intervals $(\varepsilon_m^-(\theta),\varepsilon_M^-(\theta))$ and $(\varepsilon_M^+(\theta),\varepsilon_m^+(\theta))$. For $\theta < \theta_m$, $\sigma_R(\cdot,\theta)$ has to be a monotonically increasing function with respect to strain on only two intervals, i.e., $(\varepsilon_1^*(\theta),\varepsilon_m^-(\theta)) \cup (\varepsilon_m^+(\theta),\varepsilon_2^*(\theta))$ while on the remaining one $(\varepsilon_m^-(\theta),\varepsilon_m^+(\theta))$ it is a monotonically decreasing one.

Experiments on SMAs (see for instance Otsuka et al. (1976)) show that a material in a single phase has in general a linear thermo-elastic behavior. Thus we can assume that the elastic moduli of the austenite phase (A) and martensite variants $(M^\pm)$ are constant and equal to $E_1 > 0$ and $E_3 > 0$, respectively. Moreover, we suppose here that the elastic moduli of the unstable (spinodal) regions $(I^\pm)$ are also constant and equal to $-E_2 < 0$.

Therefore for $\theta \in (\theta_m,\theta_M)$ we have

$$\sigma_R(\varepsilon,\theta) = \begin{cases} E_3(\varepsilon-\varepsilon_m^-(\theta)) + \sigma_m^-(\theta) & \text{for } \varepsilon_1^*(\theta) < \varepsilon \leqslant \varepsilon_m^-(\theta), \\ -E_2(\varepsilon-\varepsilon_m^-(\theta)) + \sigma_m^-(\theta) & \text{for } \varepsilon_m^-(\theta) < \varepsilon < \varepsilon_M^-(\theta), \\ E_1(\varepsilon-\varepsilon_M^-(\theta)) + \sigma_M^-(\theta) & \text{for } \varepsilon_M^-(\theta) \leqslant \varepsilon \leqslant \varepsilon_M^+(\theta), \\ -E_2(\varepsilon-\varepsilon_M^+(\theta)) + \sigma_M^+(\theta) & \text{for } \varepsilon_M^+(\theta) < \varepsilon < \varepsilon_m^+(\theta), \\ E_3(\varepsilon-\varepsilon_m^+(\theta)) + \sigma_m^+(\theta) & \text{for } \varepsilon_m^+(\theta) \leqslant \varepsilon < \varepsilon_2^*(\theta), \end{cases} \tag{14}$$

where according to relation (10) the following conditions have to be satisfied

$$0 < E_1 = \text{const.} < E, \qquad 0 < E_3 = \text{const.} < E. \tag{15}$$

Here the functions $\sigma_M^\pm(\theta) = \sigma_R(\varepsilon_M^\pm(\theta),\theta)$ and $\sigma_m^\pm(\theta) = \sigma_R(\varepsilon_m^\pm(\theta),\theta)$ are the local maxima and minima with respect to ε of the stress–strain curve at constant temperature. In our approach we call $\sigma = \sigma_M^\pm(\theta)$ $(\varepsilon = \varepsilon_M^\pm(\theta))$ the stress (strain) required for $(A) \to (M^\pm)$ transformations, whereas $\sigma = \sigma_m^\pm(\theta)$ $(\varepsilon = \varepsilon_m^\pm(\theta))$ the stress (strain) required for the reverse transformations $(M^\pm) \to (A)$ when $\theta \in [\theta_m,\theta_M]$.

The boundary curves $\varepsilon = \varepsilon_m^\pm(\theta)$ and $\varepsilon = \varepsilon_M^\pm(\theta)$ fix the limits of the regions of the (ε,θ)-plane on which the respective phases (A), (M^+) and (M^-) exist (see Fig. 1a), while their images through the function

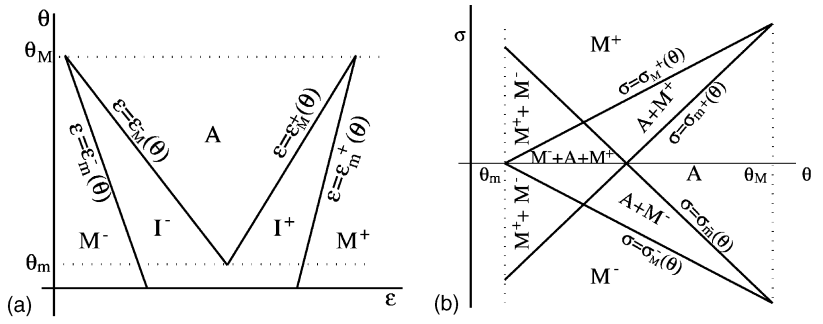

Fig. 1. (a) Austenite (A), martensite $(M^{\pm})$ and unstable $(I^{\pm})$ regions in the (ε,θ)-plane. (b) Available phases at a given (σ,θ).

$\sigma = \sigma_R(\varepsilon,\theta)$, onto the (σ,θ)-plane bound the regions which show the phases that are available to a particle at a given (σ,θ) (see Fig. 1b). The expressions of these functions and the way they are derived are explicitly given in Appendix A.

In our approach we have considered different elastic moduli for the (A) phase and martensitic variants $(M^{\pm})$, but the main difference between our stress–strain-temperature relation and that considered by Abeyaratne et al. (1994) concerns the dependence on θ of the local minima/maxima of the stress–strain curve in $(M^{+})/(M^{-})$ phases. Thus, in the paper mentioned above $\sigma_m^{+}(\theta) = E_1 M(\theta-\theta_m) - E_1(M-m)\times(\theta-\theta_M) - E_1\gamma_T$, where $\gamma_T = \text{const.} > 0$ is called the transformation strain. Consequently, the slope E_2 of the straight line connecting $(\varepsilon_M^{+}(\theta),\sigma_M^{+}(\theta))$ and $(\varepsilon_m^{+}(\theta),\sigma_m^{+}(\theta))$ is temperature-dependent, i.e., $E_2(\theta) = E_1[1-\gamma_T/(M-m)/(\theta-\theta_M)]$, becomes unbounded when $\theta\to\theta_M$ and turns σ_R into a discontinuous function.

Our approach has the advantage that it allows to extend in a continuous manner outside the interval (θ_m,θ_M) the functions $\varepsilon_M^{\pm}(\theta)$, $\varepsilon_m^{\pm}(\theta)$ and $\sigma_M^{\pm}(\theta)$, $\sigma_m^{\pm}(\theta)$ and thus to capture in a single linear description of the type (14) the thermo-mechanical considerations described at the beginning of this section for the entire range of temperature $[\theta_1^*,\theta_2^*]\supset[\theta_m,\theta_M]$.

For a better comparison with the equilibrium surface considered by Abeyaratne et al. (1994) we give bellow the explicit expression of $\sigma_R(\varepsilon,\theta)$ when $\theta\in[\theta_m,\theta_M]$ (see also Fig. 2)

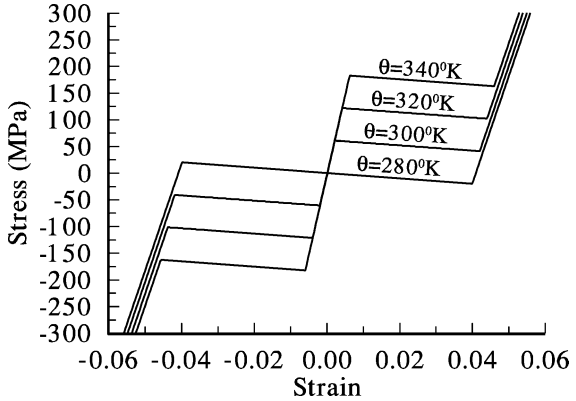

Fig. 2. Stress–strain curves at constant temperature θ described by relation (16) for the numerical entries (18).

$$\sigma_R(\varepsilon,\theta)=\begin{cases} E_3\varepsilon-E_3\alpha(\theta-\theta_T)-M(E_1-E_3)(\theta-\theta_m) & \\ -(M-m)(E_2+E_3)(\theta-\theta_M) & \text{if } \varepsilon\leqslant\varepsilon_m^-(\theta),\\ -E_2\varepsilon+E_2\alpha(\theta-\theta_T)-M(E_1+E_2)(\theta-\theta_m) & \text{if } \varepsilon\in(\varepsilon_m^-(\theta),\varepsilon_M^-(\theta)),\\ E_1\varepsilon-E_1\alpha(\theta-\theta_T) & \text{if } \varepsilon\in(\varepsilon_M^-(\theta),\varepsilon_M^+(\theta)),\\ -E_2\varepsilon+E_2\alpha(\theta-\theta_T)+M(E_1+E_2)(\theta-\theta_m) & \text{if } \varepsilon\in(\varepsilon_M^+(\theta),\varepsilon_m^+(\theta)),\\ E_3\varepsilon-E_3\alpha(\theta-\theta_T)+M(E_1-E_3)(\theta-\theta_m) & \\ +(M-m)(E_2+E_3)(\theta-\theta_M) & \text{if } \varepsilon\geqslant\varepsilon_m^+(\theta). \end{cases} \tag{16}$$

Now by using relation (11) we can explicitly determine, modulo a function $\phi(\theta)$, the free energy function for our thermo-viscoelastic model when its equilibrium stress–strain-temperature relation is described by (16). The complete expressions of the free energy function $\psi(\varepsilon,\theta,\sigma)$ of the viscoelastic model and of the equilibrium free energy function $\psi_R(\varepsilon,\theta)$ are given in Appendix B. These expressions were used through the heat propagation equation (13) in the numerical computations presented in the next section.

4. Numerical study: strain-controlled and relaxation experiments

In this section we investigate the predictions of our model in a loading–unloading strain-controlled experiment interrupted by a relaxation one. Such laboratory tests were performed in a systematic manner by Shaw and Kyriakides (1997) on a NiTi shape memory alloy and illustrate how the apparent material response is strongly influenced by the interaction between thermal and mechanical effects.

We consider a uniform bar of radius R, initially at rest, unstressed at temperature $\theta_0\in[\theta_m,\theta_M]$ for which the material is in the austenitic phase. The ambient temperature around the specimen is assumed to be constant and equal to θ_0, both ends being thermally isolated. The bar, firmly fixed at one end, is subjected to a traction–compression test with a constant velocity v^*. Between the loading and the unloading experiment we simulate a pause, during which both ends of the specimen are fixed, i.e., the length of the bar is maintained constant (relaxation experiment).

We describe the analysis associated with these loading conditions in some details while the analysis corresponding to other thermo-mechanical loadings as stress- and temperature-controlled problems will be presented elsewhere.

Thus we consider for the PDEs system $(4)_{1,2}$, $(5)_1$, (13) the following initial boundary value problem:

$$\begin{aligned} &(\varepsilon,\sigma,v,\theta)(X,0)=(0,0,0,\theta_0) \quad \text{for any } X\in[0,L],\\ &v(0,t)=v^*,\quad \theta(0,t)=\theta_0,\qquad v(L,t)=0,\quad \theta(L,t)=\theta_0 \quad \text{for any } t\in[0,t_1),\\ &v(0,t)=0,\quad \theta(0,t)=\theta_0,\qquad v(L,t)=0,\quad \theta(L,t)=\theta_0 \quad \text{for any } t\in[t_1,t_2),\\ &v(0,t)=-v^*,\quad \theta(0,t)=\theta_0,\qquad v(L,t)=0,\quad \theta(L,t)=\theta_0 \quad \text{for any } t\in[t_2,t_3). \end{aligned} \tag{17}$$

In order to study the qualitative as well as the quantitative prediction of our model we choose realistic values of the material parameters appropriate for a Cu–Zn–Ni shape memory alloy (see for instance Abeyaratne et al. (1994)). We used the following numerical entries:

$$\begin{aligned} &E=31.5\text{ GPa},\quad E_1=30\text{ GPa},\quad E_2=0.5\text{ GPa},\quad E_3=20\text{ GPa},\\ &k=10^4/\text{s},\quad \rho=8000\text{ kg/m}^3,\\ &\alpha=1.6\times10^{-6}/^\circ\text{C},\quad \kappa=20\text{ W/m/}^\circ\text{C},\quad C=500\text{ J/kg/}^\circ\text{C},\quad \omega=20\text{ W/m}^2/^\circ\text{C},\\ &\theta_m=280\ ^\circ\text{K},\quad \theta_M=10\,000\ ^\circ\text{K},\quad \theta_T=283.3\ ^\circ\text{K},\\ &M=10.1371\times10^{-5}/^\circ\text{C},\quad m=9.7253\times10^{-5}/^\circ\text{C}. \end{aligned} \tag{18}$$

The length of the bar is $L = 20$ mm, its radius $R = 2$ mm and $\theta_0 = 36.7$ °C. The experiments were performed at constant strain rates $\dot{\varepsilon}_e = v^*/L$ ranging from 5×10^{-4}/s to 5×10^{-2}/s.

For the above input data the stress required for $(A) \to (M^+)$ transformation increases at the rate $d\sigma_M(\theta)/d\theta = 3.04113$ MPa/°C, while the stress required for the reverse transformation $(M^+) \to (A)$ changes at the rate $d\sigma_m(\theta)/d\theta = 3.04114$ MPa/°C.

Like in Abeyaratne et al. (1994), the reference temperature $\theta_T \in (\theta_m, \theta_M)$ used in our numerical entries (18) has the property that the Maxwell stress for $(A) \rightleftharpoons (M)$ transformations is zero at $\theta = \theta_T$, and we call it the transformation temperature.

To obtain the numerical solution for the above initial-boundary value problem we built a first-order approximation scheme. The relation between the time integration step Δt and the mesh size ΔX is $\Delta X = \sqrt{E/\rho}\Delta t$, where Δt verifies some numerical stability conditions which will be analyzed elsewhere. In the numerical experiments presented below we have used 81 nodes on the interval $[0, L]$.

Shaw and Kyriakides (1997) were able to correlate the thermo-mechanical events of the $(A) \leftrightarrow M$ phase transformations using full field monitoring of the deformation and temperature profiles of the specimens during mechanically unstable regimes associated with the pseudoelastic material response. The same as in laboratory experiments, in order to explain the thermo-mechanical events that take place during the hysteresis loop we need to simultaneously record and examine the strain and temperature distribution in the bar as well as the end-stress $\sigma(0, t)$ versus the engineering strain $\varepsilon_e(t) = (1/L)\int_0^L \varepsilon(X, t)\, dX$. Thus, the evolution of the two phases as well as their thermal behavior is shown in the form of a 3D diagram.

4.1. Experiment at displacement rate of $\dot{\varepsilon}_e = v^*/L = 5 \times 10^{-4}\ s^{-1}$

The loading experiment lasts until $t_1 = 92.67$ s when $\sigma(0, t) = 140$ MPa and it is followed by a 10 s relaxation test. Thus, the unloading process starts at $t_2 = 102.67$ s and finishes at $t_3 = 195.35$ s when $\sigma(0, t) = 0.0$ MPa.

In this experiment the distribution of strain and temperature over the specimen was recorded at intervals of 1.0079 s and plotted as 3D diagrams in Fig. 3(b)–(d). We labeled with small circles the corresponding positions on the loading part of Fig. 3(a).

The way our model describes the pseudoelastic behavior is shown in Fig. 3(a). When loading starts, (A) phase deforms thermo-elastically until a certain transformation stress level is attained. The deformation is practically homogeneous over the entire specimen while the temperature slightly decreases about 0.009 °C except for the ends of the bar where isothermal end conditions were imposed.

Martensite nucleates for the first time inside the specimen and an increase of the temperature in the neighborhood of the transformed zone is observed (Fig. 3(b)). This event is accompanied by a drop in stress of about 7.0 MPa. Subsequently the two fronts are arrested while the temperature in the specimen dissipates through axial diffusion and radiation. Further, the martensite nucleates symmetrically at the ends of the specimen and two converging fronts separating (M^+) and (A) phases propagate through the specimen converting regions of low strain in regions of high strain. As the fronts propagate the local temperature increases as it can be seen in Fig. 3(b), while the end-stress vs. engineering strain curve exhibits a 'saw-tooth' like behavior. Each drop in load is accompanied by a sudden increase of the temperature in the transformed zone of about 1.5–2.5 °C. Although at the scale of Fig. 3(b) the transformation fronts appear to propagate with constant velocity, in reality if we look in some detail we observe that in fact they advance by small steps which accompany the oscillations of the load ('go-and-stop' strain band propagation). The propagating fronts coalesce with the stationary fronts leaving two moving fronts propagating towards each other. As they approach each other local heating intensifies due to their interaction and the local temperature at the middle of the bar briefly flares at the end of the experiment until 41.1 °C. After the specimen is entirely transformed the deformation becomes again homogeneous requiring a significant increase in stress while the temperature starts to return to ambient.

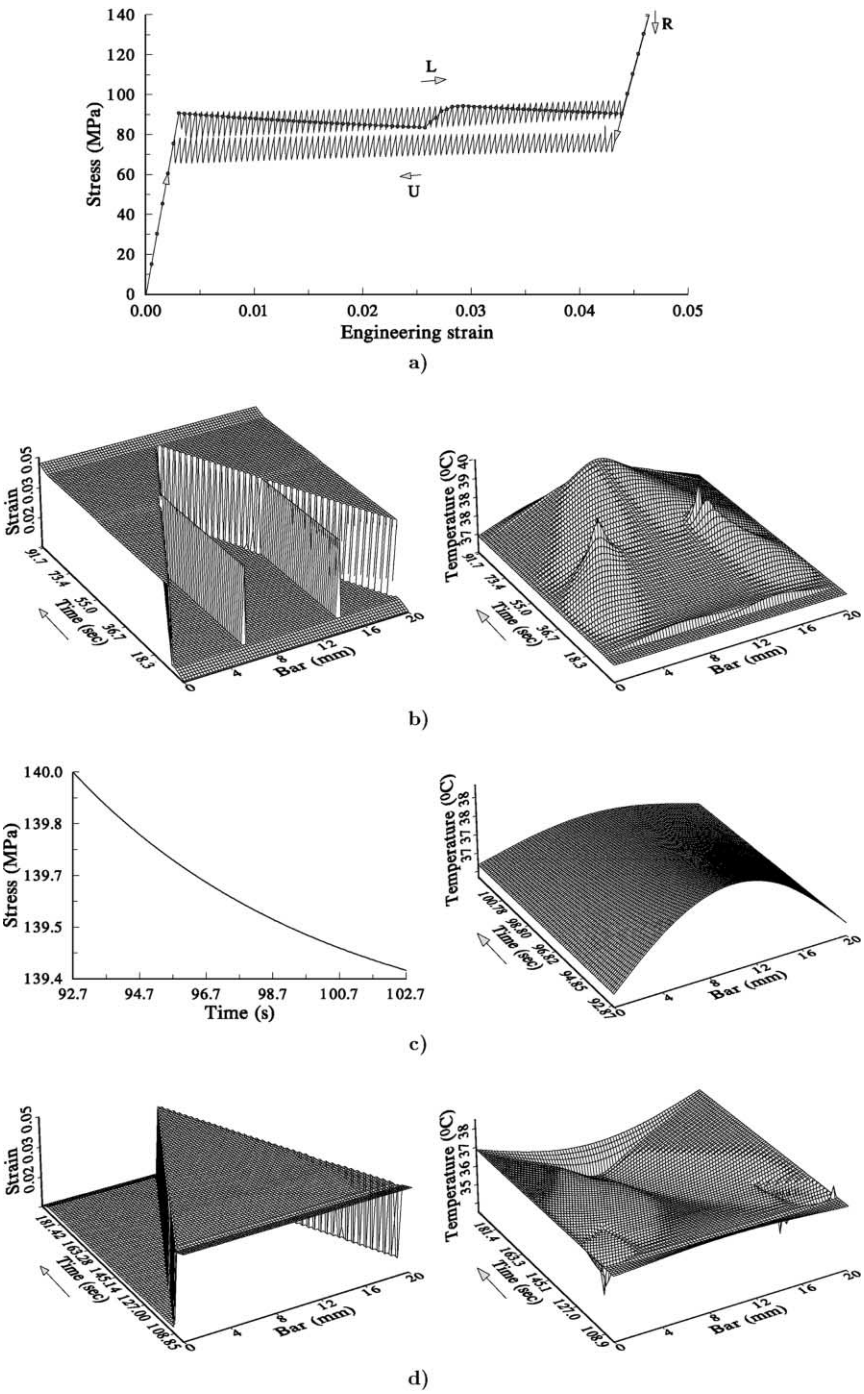

Fig. 3. Strain-controlled experiment at $\dot{\varepsilon}_e = \pm 5 \times 10^{-4}$: (a) pseudoelastic behavior; (b) $(A) \rightarrow (M^+)$ transformation and heating of the bar during loading; (c) end-stress and temperature evolution during relaxation; (d) $(M^+) \rightarrow (A)$ transformation and cooling of the bar during unloading.

Such behavior is in very good agreement with laboratory tests performed by Shaw and Kyriakides (1997) (see also Leo et al., 1993) which illustrate that the $(A) \rightarrow (M^+)$ transformation is an exothermic one.

At t_2 we simulate a pause during loading and unloading experiments maintaining fixed the ends of the bar. During this relaxation process the end-stress decreases from 140 to 139.42 MPa while the temperature decreases in the middle of the bar from 37.86 to 37 °C (Fig. 3(c)). Let us note that the relaxation of the stress as it is described by the present approach (see also Fig. 4(c)) and Fig. 6(c)) is due mainly to the thermo-mechanical coupling and to the heat transfer between the bar and its surrounding and not especially to the viscosity incorporated in the model. Relaxation processes are also predicted by the shape memory model used by Balandraud et al. (2000) (see also the references therein) when including the thermo-mechanical coupling of the material with its environment.

When the unloading test starts the stress decreases linearly and the material deforms homogeneously in the (M^+) phase without significant changes in the temperature distribution. At a low enough stress level austenite nucleates at the ends of bar where the temperature is lower with respect to the rest of the bar due to the imposed boundary conditions. Two fronts start almost simultaneously propagating towards each other at an apparent constant speed. The nucleation or propagation of (A) zones inside (M^+) zones is accompanied by a sudden raise of the stress (peaks) on the stress–engineering strain curve as can be seen in Fig. 3(a) while the local temperature briefly drops with about 1.5–2.5 °C. The temperature in the neighborhood of the propagating fronts decreases more and more as the fronts approach each other thermally interacting and attains a minimum value of 33.°C at the middle of the specimen. When the two fronts meet the whole bar has completely reverted to (A). Subsequent to this moment (A) unloads elastically, the deformation being homogeneous and the temperature returning to ambient (see Fig. 3(d)).

This proves that our model is able to describe the endothermic and non-homogeneous character of the reverse transformation as it was experimentally observed by Shaw and Kyriakides (1997) in NiTi strips.

4.2. Experiment at displacement rate of $\dot{\varepsilon}_e = v^*/L = 5 \times 10^{-3}\ s^{-1}$

In this experiment $t_1 = 9.22$ s, $t_2 = 19.22$ s, $t_3 = 28.44$ s and the time-step used to record the strain and temperature distribution over the bar is 0.10079 s. These data were used to plot the 3D diagrams in Fig. 4.

During loading (Fig. 4(b)) as well as during unloading (Fig. 4(d)) in this higher rate experiment the number of propagating fronts in the specimen is higher than in the previous one. Each $(A) \rightarrow (M^+)$/$(M^+) \rightarrow (A)$ transformed zone experiences an increase/decrease in temperature while successive 'valley'/'peaks' are observed on the stress–engineering strain curve in Fig. 4(a). As any two fronts meet the temperature momentarily flares/drops down because the corresponding zone receives/releases heat from two sides. As the fronts propagate the hot/cold zones in Fig. 4(b) and (d) spread and the local temperatures go up/down to 47.4 °C/27.2 °C at the end of the transition processes. Such an important increase/decrease in temperature (about 10 °C) is due to the fact that the heat released/absorbed by the transforming material cannot be exchanged with the exterior of the bar in such a short time interval. Finally the deformation is again homogeneous and the stress increases/decreases significantly with the slope of the elastic modulus E_3/E_1.

In this higher rate experiment the difference between the temperature of the bar at the end of the loading process and the ambient temperature is much higher than in the previous one. Consequently, during the relaxation process represented in Fig. 4(c) the end-stress decreases in 10 s with about 4 MPa, i.e., from 140 to 136.07 MPa while the temperature decreases at the middle of the bar with 6.3 °C, i.e., from 45.3 to 39 °C.

The details concerning the evolution of transformation and temperature fronts are interesting and worthy of a closer attention. Some of the observed features are described below.

Fig. 5(a) shows a zoom of the third stress-drop in Fig. 4(a). Five points are labeled successively on this curve representing the positions where the strain and temperature distribution in the bar was recorded.

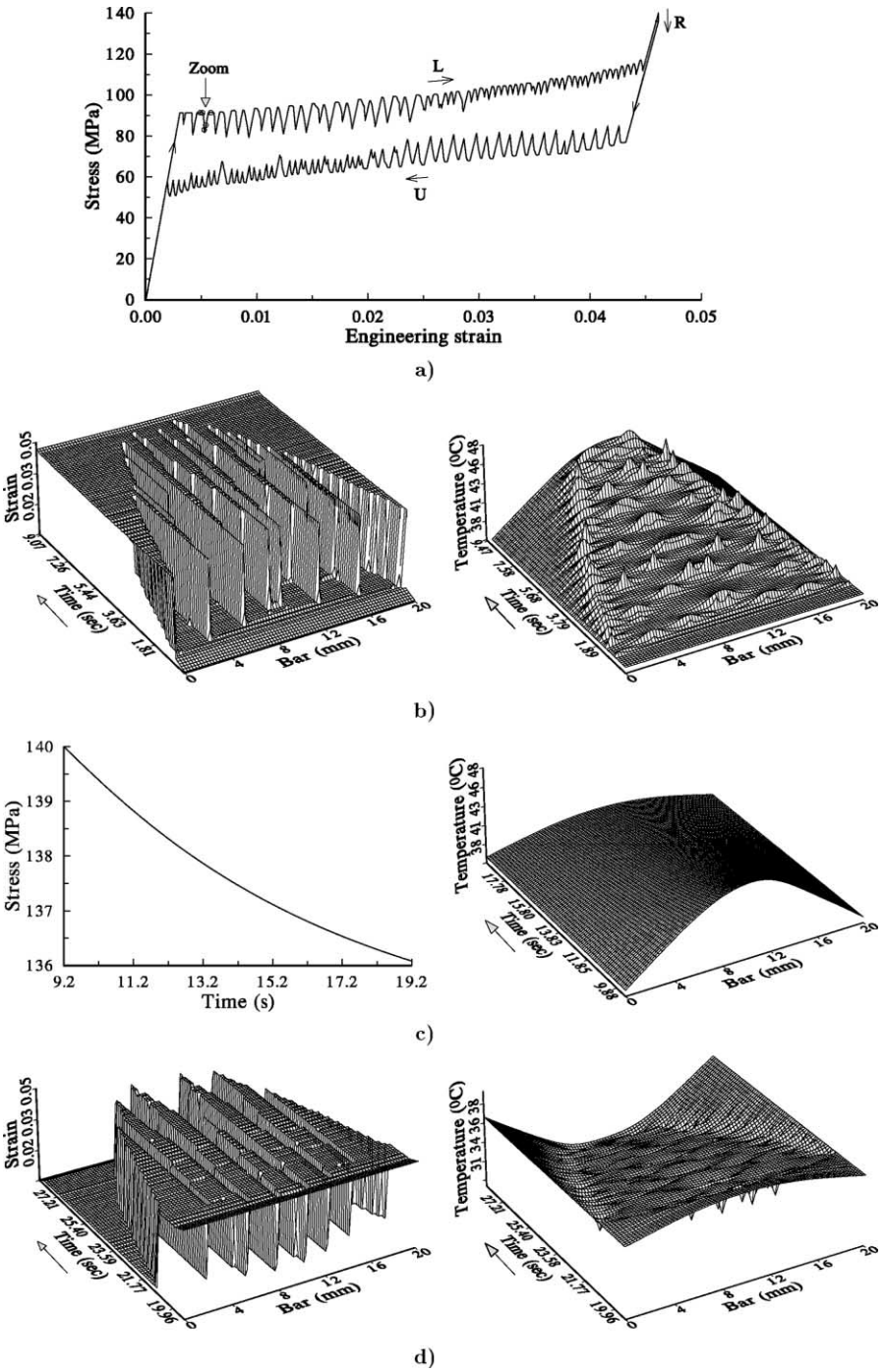

Fig. 4. Strain-controlled experiment at $\dot{\varepsilon}_e = \pm 5 \times 10^{-3}$: (a) pseudoelastic behavior; (b) $(A) \rightarrow (M^+)$ transformation and heating of the bar during loading; (c) end-stress and temperature evolution during relaxation; (d) $(M^+) \rightarrow (A)$ transformation and cooling of the bar during unloading.

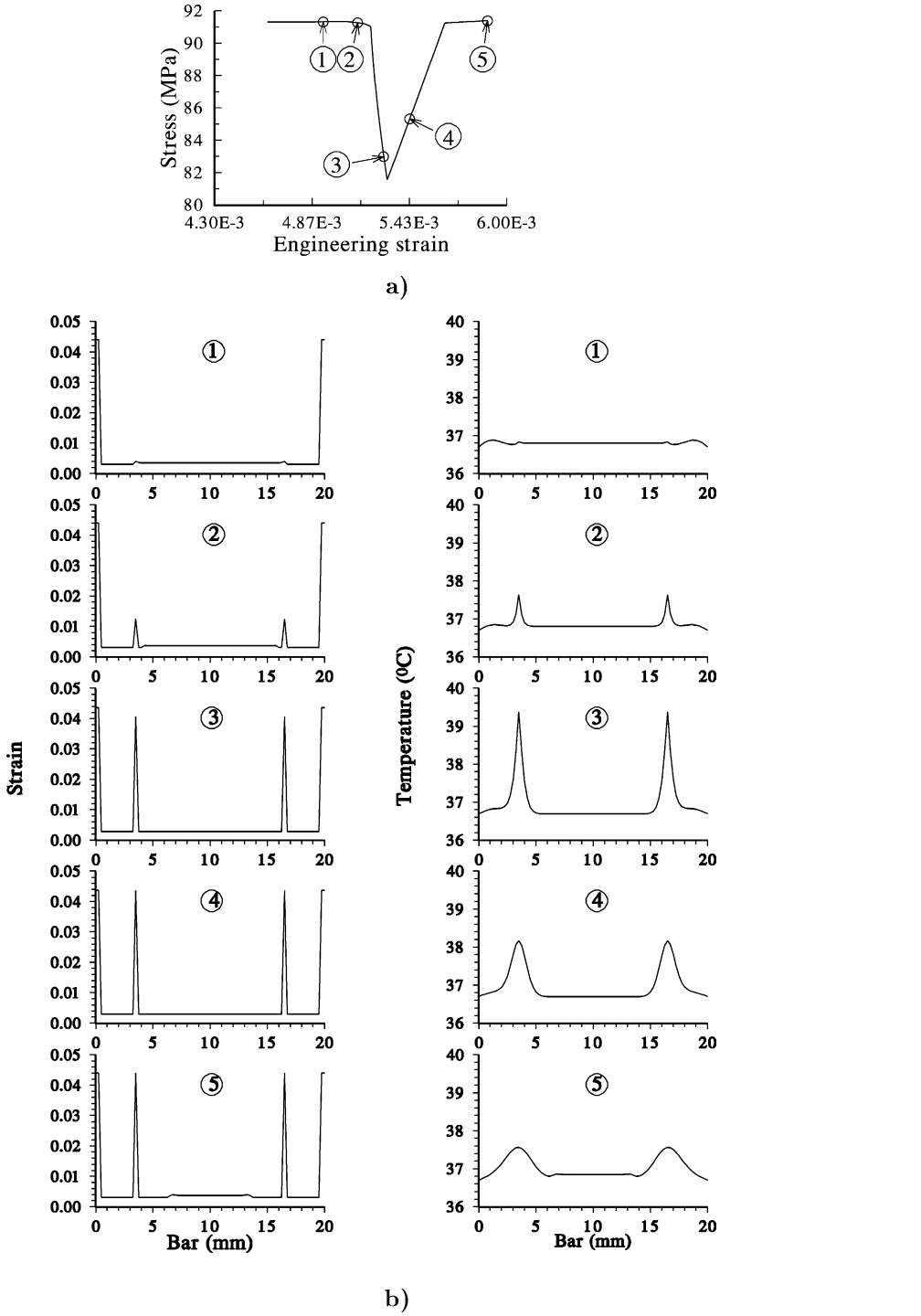

Fig. 5. Zoom of the third stress drop in Fig. 4(a) and the strain and temperature distribution at the labeled positions.

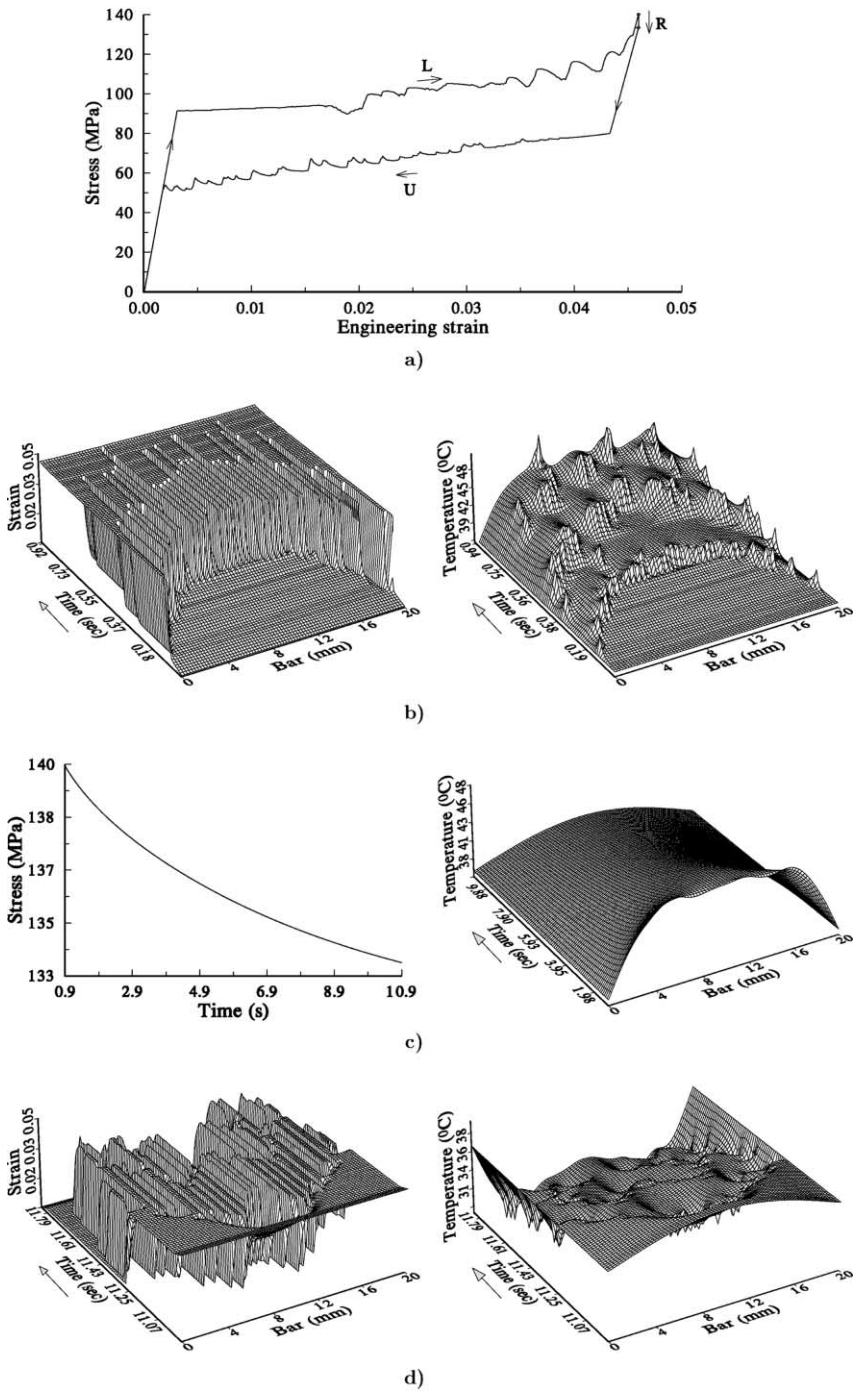

Fig. 6. Strain-controlled experiment at $\dot{\varepsilon}_e = \pm 5 \times 10^{-2}$: (a) pseudoelastic behavior; (b) $(A) \rightarrow (M^+)$ transformation and heating of the bar during loading; (c) end-stress and temperature evolution during relaxation; (d) $(M^+) \rightarrow (A)$ transformation and cooling of the bar during unloading.

The corresponding graphs are represented in Fig. 5(b). Let us note that before the stress-drop, at the position 1, martensite is localized at the ends of the bar and in their proximity the temperature is slightly increased. Moreover, we can observe the sites where the nucleation of the martensite will further appear. Thus at the position 2 the localization of strain starts to develop and the local temperature to increase. When the stress drops rapidly with 10 MPa the strain as well as the temperature in the transformed zone tend to their maximum values (see graph 3 in Fig. 5(b). Thus the local temperature increases with about 3 °C. At the beginning of the ascending part of the curve in Fig. 5(a) the localization of strain is complete and permanent while the temperature starts to dissipate in the rest of the bar through axial diffusion and to the environment through lateral radiation as can be seen on the graphs 4 and 5 in Fig. 5(b). It is useful to note that the initiation sites of the (M^+) phase can be already seen on the graphs 5 in Fig. 5(b).

This example shows that if the temperature distribution over the bar is recorded on the descending part of the 'valley' where the local temperature flares we can capture its maximum values during phase propagation. On the other hand, if the temperature distribution is recorded on the ascending part of the 'valley' where the temperature dissipates and the phase transformation fronts are arrested then we loose some information concerning the amplitude of the heating process. This situation is illustrated by Fig. 3(a). During loading the positions of the points where the temperature and strain distribution were recorded are labeled with small circles. We can see that the lower is the positions of this circles on the descending part of the valley the higher is the amplitude of the temperature of the propagating fronts. When the small circles are located on the ascending part of the 'valley' (for $\dot{\varepsilon}_e > 0.03$ in Fig. 3(a)) it is obvious that the peaks of the temperature which accompany the phase transformation process are lost and a distortion in the evolution of the temperature in Fig. 3(b) has to be observed. This is only a technical inconvenience of recording data at constant time intervals, which is similar to a laboratory situation.

What is in fact important is that our model can describe that even at the relatively slow rate test as in Fig. 5 the specimen experiences self heating in the neighborhood of the propagating transformation fronts. This is in good agreement with the physical observation that the environment could not dissipate heat at the rate that heat was being released by the transforming material (Shaw and Kyriakides, 1997).

4.3. Experiment at displacement rate of $\dot{\varepsilon}_e = v^*/L = 5 \times 10^{-2}\ s^{-1}$

This experiment could be considered a relatively high rate test and the thermal effects are more important than in the previous ones. Here $t_1 = 0.9187$ s, $t_2 = 10.9187$ s, $t_3 = 22.7562$ s and the time-step used to record the strain and temperature distribution over the bar is 0.010079 s. These recorded data were used to plot the 3D diagrams in Fig. 6.

It is obvious that multiple nucleations of the new phase appear, resulting in the coexistence and simultaneous propagation of several transformation fronts (see Fig. 6(b) and (d)). The temperature increases/decreases at the end of the loading/unloading test until 51.88 °C/26.25 °C. One can also see in Fig. 6(a) there is a closer correlation between the structure of the transformation fronts and of the temperature fronts.

Due to the sensitivity of the model to temperature during the relaxation process illustrated in Fig. 6(c) the end-stress decreases in 10 s with about 7 MPa, i.e., from 140 to 133.4 MPa while the temperature decreases at the middle of the bar with 8.7 °C, i.e., from 48.7 to 40.07 °C.

Another interesting aspect from the experimental point of view concerns the influence of the strain rate on the stress–engineering strain response. One can see that the level of the upper branch of the hysteresis loop raises for higher strain rate tests while the lower branch of the hysteresis loop descends. This effect is due mainly to the increase/decrease in temperature of the specimen as can be seen from Fig. 6(a). Consequently, one can observe that the area of the hysteresis loop increases at higher end-displacement rates.

The number of stress oscillations during loading/unloading in Fig. 3(a) corresponds to the number of nodes used. Since during a slow constant strain-rate test the amount of the nucleated phase is proportional to the amplitude of the accompanying stress drop (see Făciu, 1996) a refined mesh could lead to small and irregular serrations on the stress–engineering strain curve as those in Fig. 3(a). On the other hand a refined mesh could also lead to new locations of forming phase boundaries, but the kinetics of transformation fronts (go and stop propagation) and the global measures of the type end-stress vs. engineering strain always exhibit the same trends. A systematic study will be done elsewhere although it could be limited by the high computational effort.

Let also note that the stress fluctuations obtained in the experiments performed at higher strain rates like those in Figs. 4(a) and 6(a) are not so angular due to a higher local rate of heating/cooling and consequently to the stabilizing effects of self-heating/cooling.

5. Summary and final remarks

In this paper a new model of austenitic–martensitic phase transitions in shape memory alloy bars or wires based on a Maxwell-type viscous dissipation has been considered. In addition to inertia term and non-monotone thermoelastic stress–strain law the approach includes thermal dissipation in the form of heat conduction in the bar and convection across the lateral surface of the bar. It is a natural continuation of previous works (Suliciu, 1992; Făciu and Suliciu, 1994; Făciu, 1996) on a purely mechanical model of austenitic–martensitic phase transitions. For the thermo-viscoelastic model with Maxwellian viscosity there is a stress–strain-temperature free energy function uniquely determined by the associated thermoelastic model $\sigma = \sigma_R(\varepsilon, \theta)$, specific heat C at constant strain in the austenitic phase and the dynamic Young's modulus E. The obtained free energy function allows us to establish the appropriate heat propagation equation for our phase transforming material. Let us note that since the thermoelastic constitutive relation is only continuous in strain and temperature we get a partial differential equation with discontinuous coefficients on their domain of definition.

Numerical simulations for three constant strain-controlled rates in room temperature air were presented and they illustrate a good qualitative agreement with the full-field measurements of strain and temperature fields of Shaw and Kyriakides (1997). The number of nucleation events and the calculated evolution of strain and temperature fields combined with the stress–engineering strain response are similar to those measured in laboratory experiments. During unstable transformations, strain is clearly inhomogeneous and local dynamic effects result at end-displacement rates one might normally consider quasistatic. Due to the strong thermo-mechanical interactions heat is released or absorbed in discrete local regions.

It is worth to mention that numerical simulations of the thermo-mechanical behavior of a NiTi shape memory alloy were also considered by Shaw (2000) who used a traditional finite-plasticity constitutive model with an up–down–up trilinear stress–strain response. The irreversible nature of plasticity model limited applicability of the analysis to the $A \to M^+$ transformation during loading. Our approach has the advantage that it allows to describe both direct ($A \to M^+$) and reverse ($M^+ \to A$) transformations.

It is known that, in general, the predictions of the SMA constitutive models were investigated by neglecting inertial effects although material instabilities can be observed in the pseudoelastic behavior of certain alloys (Shaw and Kyriakides, 1997). Consequently these models are not able to acknowledge differences between stress-controlled and strain-controlled tests. Unlike these models our approach is extremely sensitive to the boundary conditions. Thus, in quasistatic strain-controlled problems it predicts serrated hysteresis loops while in stress-controlled problems it predicts non-serrated hysteresis loops (see Făciu and Mihăilescu-Suliciu, 2001b; Făciu and Suliciu, 1994) as it was observed in laboratory experiments.

Acknowledgements

The reported numerical simulations were performed using the computational facilities obtained in the framework of the Worpackage C5 of the EURROMMAT Programme ICA1-CT 2000-70022 with the European Commission.

Appendix A

We describe here the assumptions which lead us to the equilibrium stress–strain-temperature relation (16).

First, due to the symmetry of the two variants of martensite we require $\sigma_M^-(\theta) = -\sigma_M^+(\theta)$ and $\sigma_m^-(\theta) = -\sigma_m^+(\theta)$, for any $\theta \in [\theta_m, \theta_M]$. Then, since the function $\sigma = \sigma_R(\varepsilon, \theta)$ in (14) has to be continuous we get

$$\sigma_M^+(\theta) = \frac{E_1}{2}(\varepsilon_M^+(\theta) - \varepsilon_M^-(\theta)), \quad \sigma_m^+(\theta) = E_2(\varepsilon_m^-(\theta) - \varepsilon_M^-(\theta)) + \frac{E_1}{2}(\varepsilon_M^+(\theta) - \varepsilon_M^-(\theta)). \tag{A.1}$$

In order that relation (14) describes a piecewise linear thermoelastic behavior we require the functions $\varepsilon = \varepsilon_m^{\pm}(\theta)$ and $\varepsilon = \varepsilon_M^{\pm}(\theta)$ to be linear in θ as well as the functions $\sigma = \sigma_m^{\pm}(\theta)$ and $\sigma = \sigma_M^{\pm}(\theta)$. Moreover, according to our previous thermo-mechanical assumptions (see Fig. 1), they have to satisfy the following conditions: $\sigma_M^+(\theta_M) = \sigma_m^+(\theta_M)$, $\varepsilon_M^+(\theta_M) = \varepsilon_m^+(\theta_M)$, $\varepsilon_M^-(\theta_M) = \varepsilon_m^-(\theta_M)$, $\sigma_M^+(\theta_m) = 0$, and $\varepsilon_M^+(\theta_m) = \varepsilon_M^-(\theta_m)$.

Now by assuming that the undeformed material in the (A) phase is stress-free at a reference temperature θ_T, i.e., $\sigma_R(0, \theta_T) = 0$ we get

$$\begin{aligned} &\varepsilon_M^+(\theta) = \alpha(\theta - \theta_T) + M(\theta - \theta_m), \quad \varepsilon_m^+(\theta) = \alpha(\theta - \theta_T) - (M - m)(\theta - \theta_M) + M(\theta - \theta_m), \\ &\varepsilon_M^-(\theta) = \alpha(\theta - \theta_T) - M(\theta - \theta_m), \quad \varepsilon_m^-(\theta) = \alpha(\theta - \theta_T) + (M - m)(\theta - \theta_M) - M(\theta - \theta_m) \end{aligned} \tag{A.2}$$

and

$$\begin{aligned} &\sigma_M^+(\theta) = -\sigma_M^-(\theta) = E_1 M(\theta - \theta_m), \\ &\sigma_m^+(\theta) = -\sigma_m^-(\theta) = E_2(M - m)(\theta - \theta_M) + E_1 M(\theta - \theta_m), \end{aligned} \tag{A.3}$$

where $\alpha = \text{const.} > 0$ is the thermal expansion coefficient of the material in phase (A) and $M = \text{const.} > 0$, $m = \text{const.} > 0$ are other two material constants.

Since the boundaries of the (A), (M^+) and (M^-) regions in the (ε, θ) plane have to satisfy the inequalities

$$\begin{aligned} &-1 < \varepsilon_m^-(\theta) < \varepsilon_M^-(\theta) < \varepsilon_M^+(\theta) < \varepsilon_m^+(\theta) \quad \text{for any } \theta \in (\theta_m, \theta_M), \\ &-1 < \varepsilon_m^-(\theta) < \varepsilon_m^+(\theta) \quad \text{for any } \theta_1^* < \theta < \theta_m, \end{aligned} \tag{A.4}$$

we derive the following restrictions on the material parameters entering (A.2) and (A.3)

$$0 < \alpha < m < M, \quad \alpha(\theta_M - \theta_T) - M(\theta_M - \theta_m) > -1. \tag{A.5}$$

Let us specify the meaning of the two constants m and M. It is known that one can experimentally determine the dependence of nucleation stress on temperature (see for instance Fig. 7 in Shaw and Kyriakides (1997)). According to relations (A.3), $E_1 M$ and $E_1 M + E_2(M - m)$ describe the rate at which the stress required for $(A) \to (M^+)$ and $(M^+) \to (A)$ transformations, respectively, vary with respect to the temperature. Thus the two constants m and M may be determined when the elastic moduli E_i, $i = 1, 2, 3$ are already known.

Appendix B

In this section we give a brief description of the free-energy function of the thermo-viscoelastic model $(5)_1$ for the equilibrium stress–strain-temperature relation (16).

Let us note that according to (11) the equilibrium free energy function is given by

$$\varrho\hat{\psi}_R(\varepsilon,\theta)=\int_0^{\varepsilon}\sigma_R(s,\theta)\,\mathrm{d}s+\phi(\theta). \tag{B.1}$$

We determine the unknown function of temperature $\phi(\theta)$ in (B.1) (and (11)) by assuming that the specific heat at constant strain of the thermoelastic material $\sigma=\sigma_R(\varepsilon,\theta)$ is constant in the austenitic phase, i.e.,

$$-\theta\frac{\partial^2\hat{\psi}_R}{\partial\theta^2}(\varepsilon,\theta)=C=\text{const.}\quad\text{for }\varepsilon\in(\varepsilon_M^-(\theta),\varepsilon_M^+(\theta)), \tag{B.2}$$

From (B.1) and (B.2) we obtain

$$\phi(\theta)=\varrho\hat{\psi}_R(\varepsilon_0,\tilde{\theta})+\varrho(\theta-\tilde{\theta})(C-\hat{\eta}_R(\varepsilon_0,\tilde{\theta}))-\varrho C\theta\ln(\theta/\tilde{\theta}), \tag{B.3}$$

where $\varepsilon_0\equiv\varepsilon_M^{\pm}(\theta_m)=\alpha(\theta_m-\theta_T)$ is the only strain value which belongs to the austenitic phase for any $\theta\in[\theta_m,\theta_M]$ and $\tilde{\theta}\in[\theta_1^*,\theta_2^*]$ is an arbitrarily fixed value of the temperature. If we choose for instance $\tilde{\theta}=\theta_T$, $\rho\hat{\psi}_R(\varepsilon_0,\theta_T)=\theta_T C$ and $\hat{\eta}_R(\varepsilon_0,\theta_T)=0$ then the expression of $\hat{\psi}_R(\varepsilon,\theta)$ on the intervals corresponding to phases (A), (M^+) and the spinodal region (I^+) for the proposed equilibrium surface (16) when $\theta\in[\theta_m,\theta_M]$ is

$$\varrho\hat{\psi}_R(\varepsilon,\theta)=\varrho\theta C(1-\ln(\theta/\theta_T))+\begin{cases}\frac{E_1}{2}\varepsilon^2-E_1\alpha(\theta-\theta_T)\varepsilon\quad\text{for }\varepsilon\in[\varepsilon_M^-(\theta),\varepsilon_M^+(\theta)],\\ \frac{-E_2}{2}\varepsilon^2+[E_2\alpha(\theta-\theta_T)+M(E_1+E_2)(\theta-\theta_m)]\varepsilon+\chi_1(\theta)\\ \quad\text{for }\varepsilon\in(\varepsilon_M^+(\theta),\varepsilon_m^+(\theta)),\\ \frac{E_3}{2}\varepsilon^2-[E_3\alpha(\theta-\theta_T)-(E_2+E_3)(M-m)(\theta-\theta_M)\\ \quad-(E_1-E_3)M(\theta-\theta_m)]\varepsilon+\chi_2(\theta)\\ \quad\text{for }\varepsilon\in[\varepsilon_m^+(\theta),\varepsilon_2^*(\theta)),\end{cases} \tag{B.4}$$

where

$$\begin{aligned}\chi_1(\theta)&=-\frac{(E_1+E_2)}{2}[\alpha(\theta-\theta_T)+M(\theta-\theta_m)]^2,\\ \chi_2(\theta)&=\frac{(E_3-E_1)}{2}[\alpha(\theta-\theta_T)+M(\theta-\theta_m)]^2-(M-m)(E_2+E_3)(\theta-\theta_M)\\ &\quad\times\left[\alpha(\theta-\theta_T)+M(\theta-\theta_m)-\frac{(M-m)}{2}(\theta-\theta_M)\right].\end{aligned} \tag{B.5}$$

Let us note that the coefficient of thermal expansion of the thermoelastic constitutive equation we propose here, i.e. $-\frac{\partial^2\hat{\psi}_R}{\partial\varepsilon\partial\theta}\Big/\frac{\partial^2\hat{\psi}_R}{\partial\varepsilon^2}$, is a piecewise constant function on its domain of definition. For instance, on the (A)-region $(\varepsilon\in[\varepsilon_M^-(\theta),\varepsilon_M^+(\theta)])$ it is equal to α, on (I^+)-region $(\varepsilon\in[\varepsilon_M^+(\theta),\varepsilon_m^+(\theta)])$, it is equal to $\alpha+M(1+E_1/E_2)$, while on (M^+)-region $(\varepsilon>\varepsilon_m^+(\theta))$ it is equal to $\alpha+m(E_3+E_2)/E_3-M(E_1+E_2)/E_3$. The specific heat function at constant strain is also discontinuous and has for example the following values:

$$-\theta\frac{\partial^2\psi_R}{\partial\theta^2}=\begin{cases}C & \text{for }\varepsilon\in[\varepsilon_M^-(\theta),\varepsilon_M^+(\theta)],\\ C+\frac{(E_1+E_2)}{\varrho}(\alpha+M)^2\theta & \text{for }\varepsilon\in(\varepsilon_M^+(\theta),\varepsilon_m^+(\theta)),\\ C+[\frac{(E_1-E_2)}{\varrho}(\alpha+M)^2+\frac{(E_2+E_3)}{\varrho}(M-m)(M+m+2\alpha)]\theta & \text{for }\varepsilon\in[\varepsilon_m^+(\theta),\varepsilon_2^*(\theta)).\end{cases} \tag{B.6}$$

Since in this paper we only investigate the capability of the model to describe stress-induced $(A) \rightleftharpoons (M^+)$ phase transitions we give bellow a partial description of the free energy function $\psi = \hat{\psi}(\varepsilon, \sigma, \theta)$ of the thermo-viscoelastic model as it was deduced by Făciu and Mihăilescu-Suliciu (2001a):

$$\hat{\varrho}\psi(\varepsilon,\sigma,\theta) = \frac{\sigma^2}{2E} + \frac{E_1^2\alpha^2}{2(E-E_1)}(\theta-\theta_T)^2 + \varrho\theta C(1-\ln(\theta/\theta_T)) + \begin{cases} \frac{E_1}{2E(E-E_1)}(\sigma-E\varepsilon)^2 + \frac{E_1\alpha^2}{(E-E_1)}(\theta-\theta_T)(\sigma-E\varepsilon) & \text{for } \tau_M^+(\theta) \leqslant \sigma - E\varepsilon \leqslant \tau_M^-(\theta), \\ -\frac{E_2}{2E(E+E_2)}(\sigma-E\varepsilon)^2 + \varphi_1(\theta) & \\ \quad -\left[\frac{E_2\alpha}{(E+E_2)}(\theta-\theta_T) + \frac{(E_1+E_2)M}{(E+E_2)}(\theta-\theta_m)\right](\sigma-E\varepsilon) & \text{for } \tau_m^+(\theta) < \sigma - E\varepsilon < \tau_M^+(\theta), \\ \frac{E_3}{2E(E-E_3)}(\sigma-E\varepsilon)^2 + \varphi_2(\theta) + \frac{(\sigma-E\varepsilon)}{(E-E_3)}[E_3\alpha(\theta-\theta_T) & \\ \quad -(E_2+E_3)(M-m)(\theta-\theta_M) - (E_1-E_3)M(\theta-\theta_m)] & \text{for } \sigma - E\varepsilon \leqslant \tau_m^+(\theta), \end{cases} \tag{B.7}$$

where

$$\begin{aligned} \varphi_1(\theta) &= -\frac{(E_1+E_2)}{2(E+E_2)(E-E_1)}[E\alpha(\theta-\theta_T) + M(E-E_1)(\theta-\theta_m)]^2, \\ \varphi_2(\theta) &= \varphi_1(\theta) + \frac{(E_2+E_3)}{2(E+E_2)(E-E_3)}[E\alpha(\theta-\theta_T) + M(E-E_1)(\theta-\theta_m) - (M-m)(E+E_2)(\theta-\theta_M)]^2 \end{aligned} \tag{B.8}$$

and

$$\begin{aligned} \tau_M^-(\theta) &= M(E-E_1)(\theta-\theta_m) - E\alpha(\theta-\theta_T), \\ \tau_M^+(\theta) &= -M(E-E_1)(\theta-\theta_m) - E\alpha(\theta-\theta_T), \\ \tau_m^+(\theta) &= \tau_M^+(\theta) + (\theta-\theta_M)(M-m)(E+E_2). \end{aligned} \tag{B.9}$$

References

Abeyaratne, R., Knowles, J.K., 1991. Implications of viscosity and strain-gradient effects for the kinetics of propagating phase boundaries in solids. SIAM J. Appl. Math. 51, 1205–1221.

Abeyaratne, R., Knowles, J.K., 1993. A continuum model of a thermoelastic solid capable of undergoing phase transitions. J. Mech. Phys. Solids 41, 541–571.

Abeyaratne, R., Kim, S.-J., Knowles, J.K., 1994. A one-dimensional continuum model for shape memory alloys. Int. J. Solids Struct. 31, 2229–2249.

Balandraud, X., Ernst, E., Soós, E., 2000. Relaxation and creep phenomena in shape memory alloys. Part I: Hysteresis loop and pseudoelastic behavior. Part II: Stress relaxation and strain creep during phase transformation. Z. Angew. Math. Phys. 51, 171–203, 419–448.

Ball, J.M., James, R.D., 1987. Fine phase mixtures as minimizers of energy. Arch. Rat. Mech. Anal. 100, 13–52.

Ericksen, J.L., 1975. Equilibrium of bars. J. Elasticity 5, 191–201.

Făciu, C., 1991. Numerical aspects in modelling phase transitions by rate-type constitutive equations. Int. J. Eng. Sci. 29, 1103–1119.

Făciu, C., 1996. Initiation and growth of strain bands in rate-type viscoelastic materials. Part I: Discontinuous strain solutions. Part II: The energetics of the banding mechanism. Eur. J. Mech. A/Solids 15, 969–988, 989–1011.

Făciu, C., Suliciu, I., 1994. A Maxwellian model for pseudoelastic materials. Scripta Metall. Mater. 31, 1399–1404.

Făciu, C., Mihăilescu-Suliciu, M., 1987. The energy in one-dimensional rate-type semilinear viscoelasticity. Int. J. Solids Struct. 23, 1505–1520.

Făciu, C., Mihăilescu-Suliciu, M., 2001a. A Maxwellian thermo-viscoelastic model for shape memory alloys. An energetic study (submitted).

Făciu, C., Mihăilescu-Suliciu, M., 2001b. On a rate-type thermo-mechanical model for shape memory bars. Stress-controlled problems. In: Proceedings of the Workshop on Shape Memory Alloy Materials, Warsaw, Poland, September 3–6, 2001.

James, R.D., 1981. Finite deformation by mechanical twinning. Arch. Rat. Mech. Anal. 77, 143–176.

Lin, P.H., Tobushi, H., Tanaka, K., Hattori, T., Ikai, A., 1994. Influence of strain rate on deformation properties of TiNi shape memory alloy. Trans. Jpn. Soc. Mech. Eng. (A) 60, 1837–1842.

Leo, P.H., Shield, T., Bruno, O.P., 1993. Transient heat transfer effects on the pseudoelastic behavior of shape memory wires. Acta Metall. Mater. 41, 2477–2485.

Mihăilescu-Suliciu, M., Suliciu, I., 1993. Stable numerical solutions to a dynamic problem for a softening material. Mech. Res. Commun. 20, 475–480.

Otsuka, K., Wayman, C.M. (Eds.), 1998. Shape Memory Materials. Cambridge University Press, Cambridge.

Otsuka, K., Wayman, C.M., Nakai, K., Sakamoto, H., Shimizu, K., 1976. Superelasticity effects and stress-induced martensitic transformations in Cu–Al–Ni alloys. Acta Metall. Mater. 24, 207–226.

Pego, R., 1987. Phase transitions in one-dimensional nonlinear viscoelasticity: admissibility and stability. Arch. Rat. Mech. Anal. 97, 353–394.

Shaw, J.A., Kyriakides, S., 1997. On the nucleation and propagation of phase transformation fronts in a NiTi alloy. Acta Mater. 45, 683–700.

Shaw, J.A., 2000. Simulations of localized thermo-mechanical behavior in a NiTi shape memory alloy. Int. J. Plasticity 16, 541–562.

Suliciu, I., 1989. On the description of the dynamics of phase transitions by means of rate-type constitutive equations. A model problem. In: Khan, A.S., Tokuda, M. (Eds.), Plasticity '89. Pergamon Press, New York, pp. 417–420.

Suliciu, I., 1992. Some stability–instability problems in phase transitions modelled by piecewise linear elastic or viscoelastic constitutive equations. Int. J. Eng. Sci. 30, 483–494.

Suliciu, I., 1998. Energy estimates in rate-type thermo-viscoplasticity. Int. J. Plasticity 14, 227–244.

Vainchtein, A., 2001. Thermodynamics of martensitic phase transitions and hysteresis (this volume).

Vainchtein, A., Rosakis, P., 1999. Hysteresis and stick-slip motion of phase boundaries in dynamic models of phase transitions. J. Nonlinear Sci. 9, 697–719.